

# Three Dimensional Imaging for Magnetohydrodynamic Computations

Roberto Lionello

Email: [lionel@arcetri.astro.it](mailto:lionel@arcetri.astro.it)

WWW: <http://www.arcetri.astro.it/~lionel>

Dipartimento di Astronomia e Scienza dello Spazio

Università degli Studi di Firenze,

Largo Enrico Fermi 5, I-50125 Firenze, Italy

## Abstract

Data produced by three dimensional MHD calculations are often difficult to visualize. Here we present a technique to view field lines of vector fields and one to display multiple isosurfaces of scalar fields. These methods do not rely on expensive commercial software and are general enough to be applied to other research sectors where visualization of 3D fields is important. Printed copies of the images are easily obtainable with ordinary printers. An optional procedure, to facilitate comparison with observations and consequently of more limited application field, is also discussed.

## 1. Introduction

In order to study the physics of coronal loops in the Sun, we are currently performing simulations with a computer code which solves the resistive and viscous magnetohydrodynamic (MHD hereafter) equations in cylindrical geometry [LMS96].

Loops made of tenuous and magnetized plasma are often observed in the hot environment of the solar corona, while their ends are rooted in the photosphere below. A considerable amount of energy can be released during loop instabilities which might explain the large variety of activity manifestations of different energetical importance observed in a solar active region, ranging from heating to large flares [P82].

A sketch of the coordinate system, used to simulate the evolution of instabilities in coronal loops, is presented in Fig. 1. Note that we have ignored the curvature of the loops, which appear to have been “straightened out”. During the runs of the code, at every fixed interval of time, data describing both vector fields (magnetic field, velocity) and scalar fields (pressure, density) are saved on disk. Many other physical quantities (typically the current density, the temperature and so on) can be calculated from those data, if they are needed.

Visualizing three dimensional images is always challenging, even when sophisticated commercial software is available. In the context of solar MHD, presentation of results has been limited for a long time to two-dimensional cuts of 3D scalar fields or confusing bundles of force lines of vector fields. Quite recently authors have exploited several packages to visualize the results of their simulations, and they have obtained much better results. Dahlburg and Antiochos

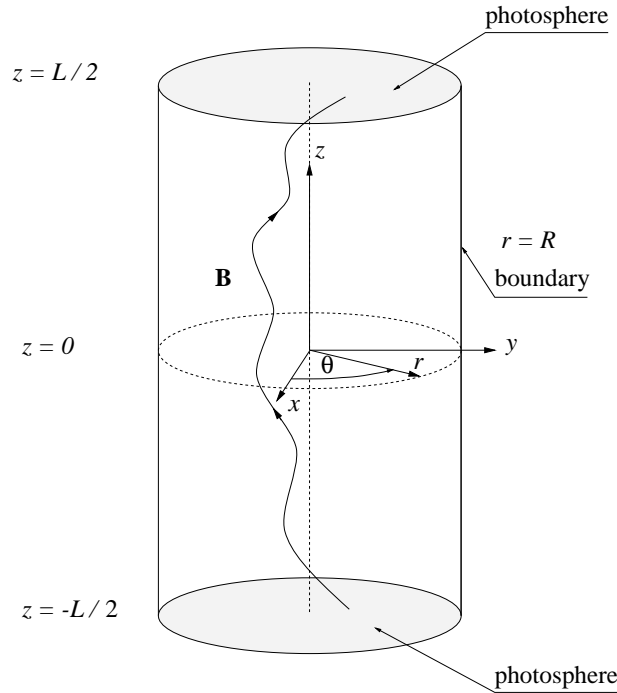


Figure 1: Coordinates and boundaries for modeling coronal loops. Field lines are anchored in the photosphere at  $z = \pm L/2$ . Curvature observed in real loops is ignored during computations. In the present paper the Cartesian coordinates  $(x, y, z)$  are used.

[DA95] used Flow Analysis Software Toolkit (FAST), which was developed at NASA Ames Research Center, to show isosurfaces of the magnetic field magnitude. Galsgaard and Nordlund [GN96] plotted isosurfaces of the magnetic field intensity and magnetic field line traces using IDL and NAG Explorer. Beliën *et al.* [BPSLG96] used the visualization package Data eXplorer (DX) produced by IBM to simulate soft X-ray emission in solar coronal loops. Beliën and Leenders [BL96] presented a comparison of different commercial visualization packages applied to plasma physics. However the cost of such image processing tools and their hardware requirements can sometimes be an obstacle.

Here we provide the reader with simple methods to view three dimensional fields. These techniques do not depend on expensive proprietary software and their application range is not restricted to the presentation of the data produced by our code (or of quantities relevant to plasma astrophysics in general). In fact they can be used with any scalar field, with any vector field (of which we can compute field lines) and in any geometry. A clear and comprehensive vision of our data ensues from our methods, allowing better understanding of the physical processes that are driving the evolution of the system. Moreover good quality hard copies of the images can be obtained with common black and white laser printers. Even if our code works in cylindrical coordinates, for convenience in the present paper we shall always use Cartesian coordinates.

In Section 2. we discuss how to implement a method to view field lines with the help of a software capable of plotting segments in grey tones. In Section 3. we explain how to display isosurfaces of scalar fields in three dimensions using non-commercial software. Section 4. contains conclusions. In the Appendix details regarding an optional procedure to restore “straightened out” loops to their original curved shape are discussed.

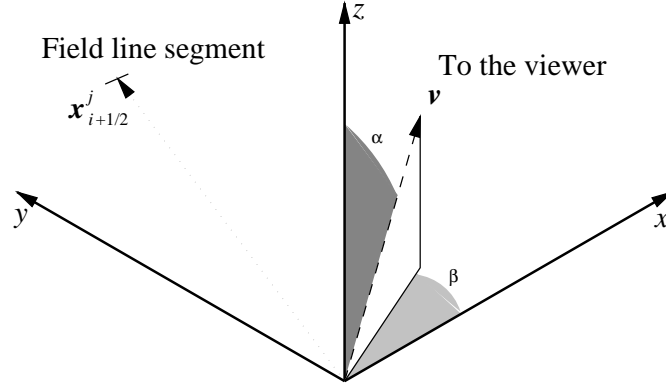


Figure 2: Frame of reference in which we plot field lines.  $\mathbf{x}_{i+1/2}^j$  is the medium point of one of the segments composing the field lines. Segments are sorted according to the value of scalar product with the vector  $\mathbf{v}$ , which indicates the direction towards the viewer. Then they are plotted in grey tones, the darker being the farther.

## 2. Plotting Field Lines

Many field line plots, which are often found in the literature, are rather confusing than enlightening. In fact, authors generally trace black field lines over a white background. That is not an adequate method to create an illusion of depth. In order to obtain better pictures (and better physical insight), we have developed a technique that takes advantage of a gray tone scale over a black background. Someone may also appreciate our technique because color pictures are often more expensive and demand more sophisticated hardware, if high quality is to be obtained.

Let us consider a vector field  $\mathbf{B}$  (in our case this is the magnetic field). We can calculate the field lines of  $\mathbf{B}$  by solving the following ordinary differential equation:

$$\begin{aligned} \frac{d\mathbf{x}}{ds} &= \frac{\mathbf{B}(\mathbf{x})}{\|\mathbf{B}\|}, \\ ds &= \|\mathbf{dx}\|. \end{aligned} \quad (1)$$

Where  $\mathbf{x} \equiv (x, y, z)$  is the position vector,  $s$  is the distance measured along the field line and  $\|\dots\|$  indicates the Euclidean norm. We solve Eq. (1) numerically with a standard Runge-Kutta scheme. This yields each field line as a set of points  $\mathbf{x}_0, \mathbf{x}_1, \dots, \mathbf{x}_N$ .

The next step is usually to connect neighboring points with segments to obtain a field line. We prefer to perform a fast treatment on our data that will permit us to produce a much clearer result. Let  $M$  be the number of field lines (each composed of  $N_j$  segments,  $j = 1, \dots, M$ ) that we intend to plot. We indicate with  $\mathbf{v}$  (see Fig. 2) a fixed vector pointing towards the viewer.  $\mathbf{v}$  can be expressed, with the help of the polar and azimuthal angles  $\alpha$  and  $\beta$ , as

$$\mathbf{v} = (\cos \beta \sin \alpha, \sin \beta \sin \alpha, \cos \alpha) \quad (2)$$

Let  $\mathbf{x}_{i+1/2}^j$  be the median point of the  $(i+1)$ th segment of the  $j$ th field line,  $[\mathbf{x}_i^j, \mathbf{x}_{i+1}^j]$ . We sort all the segments, which compose the field lines, according to the value of the scalar product

$$S_i^j = \mathbf{v} \cdot \mathbf{x}_{i+1/2}^j, \quad (3)$$

in increasing order. To each segment we associate a grey tone value

$$V_i^j = \frac{S_i^j - S_{\min} + \epsilon}{S_{\max} - S_{\min} + \epsilon}. \quad (4)$$

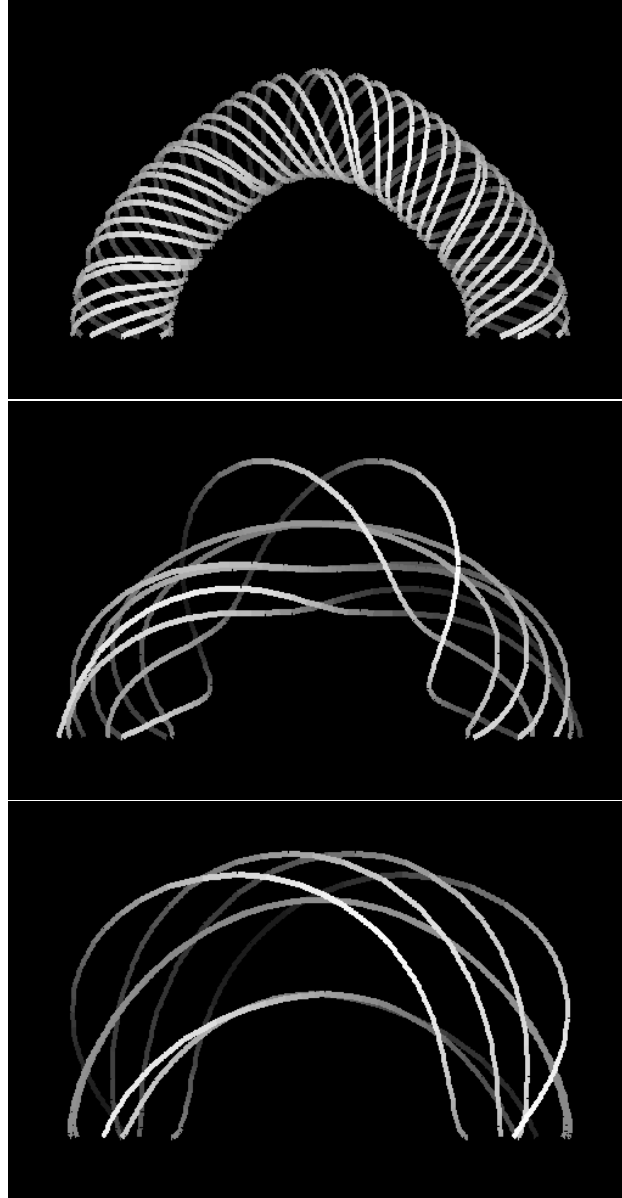


Figure 3: Magnetic field lines at three instants ( $t = 120, 150$  and  $180$  times) during the nonlinear phase of a kink instability in a coronal loop. Magnetic reconnection is taking place. Notice the almost complete disappearance of the azimuthal component of the magnetic field: a great amount of energy is released during this phase.

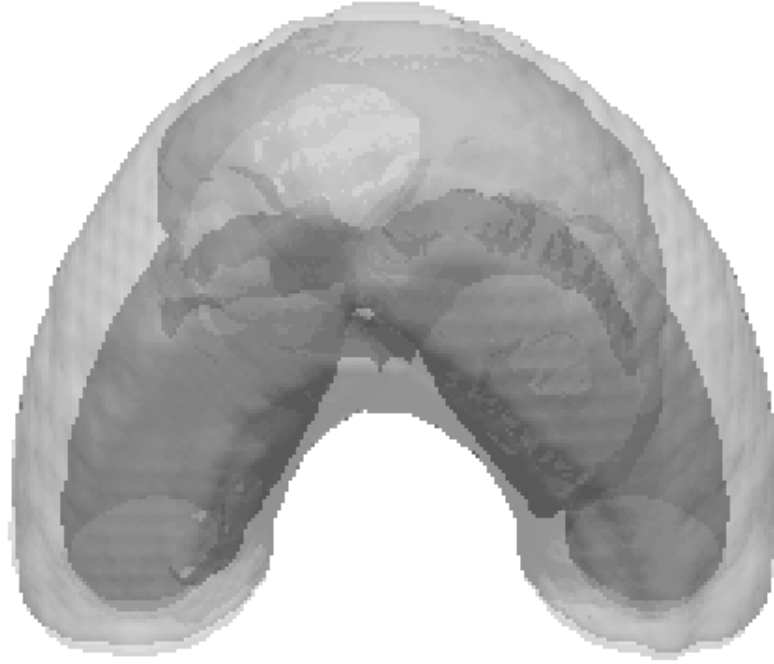


Figure 4: Three levels of temperatures during the nonlinear phase of a kink instability in coronal loop. It is the same simulation shown in Fig. 3. Time is  $t = 130$  Alfvén times.

Where  $\epsilon$  is a small positive number that prevents the tracing of black segments ( $V = 0$  is black and  $V = 1$  is white). Then we can plot all the segments in the established order. Gray tone field lines before a black background will appear, the segments which are farther from the observer being darker.

To fully appreciate the advantages of our technique, we present in Fig. 3 a sequence of three snapshots taken at  $t = 120, 150$  and  $180$  Alfvén times, depicting the magnetic field lines during the nonlinear phase of a kink instability in a coronal loop [ELV96, VLE96]. The point of view is  $\mathbf{v} = (0, -1, 0)$ . Field line points have been remapped from a cylindrical to a toroidal configuration (see the Appendix), in order to provide a more intuitive presentation of coronal loops. Magnetic reconnection takes place at the center of the loop (see also Fig. 4). The azimuthal component of the magnetic field is almost completely dissipated and a considerable amount of energy is thus released, enough for a small flare.

The method described in this section can be easily implemented in any high-level language or computing environment. Furthermore it requires negligible computational time to produce clear and accurate pictures of field lines.

### 3. Viewing Multiple Isosurfaces

Several software packages allows us to plot isosurfaces of three dimensional scalar fields. However it is often difficult (or even impossible) to obtain a satisfactory representation of more isosurfaces, related to different intensities of a scalar field, in a single picture. Here we demonstrate how it is possible to display up to three isosurfaces simultaneously using a copyrighted freeware

program, Persistence of Vision Ray Tracer (or POV-Ray)<sup>1</sup>.

POV-Ray is a powerful software, which is able to create a three dimensional image from a text file in which we specify the shape and light propagation properties of the objects we want to render, the point of view, and the luminous source(s) [P93].

It is possible to produce an isosurface using a POV-Ray primitive called `blob`. A `blob` is composed of  $N$  points  $\mathbf{p}_i = (x_i, y_i, z_i)$ , with which a normalization radius  $a_i$ , and a “strength”  $s_i$  are associated. The latter parameters refer to a “density”  $d_i$ , whose value is different from zero only within a distance  $a_i$  from  $\mathbf{p}_i$  and equal to

$$d_i(x, y, z) = s_i \left[ 1 - \frac{(x - x_i)^2 + (y - y_i)^2 + (z - z_i)^2}{a_i^2} \right]^2. \quad (5)$$

For a generic point in space, POV-Ray sums the individual component densities,

$$d = \sum_{i=1}^N d_i, \quad (6)$$

and looks for the regions where  $d$  is equal to a “threshold” value, which is the intensity of the isosurface we wish to plot.

Hence to generate an image either in toroidal or cylindrical configuration (as explained in the Appendix), we first set up a regularly spaced grid. Then we fix a threshold intensity and we test at each grid node if  $s_i$  is greater than the threshold. In case of positive response, we write the `blob` components in a text file. We found that the exact value of  $a_i$  is not critical, as long as it is chosen about twice the grid spacing and the grid resolution is adequately fine. Next, a point of view and a light source are added to the file. Eventually, the `blob` can be displayed with POV-Ray.

If we wish to, we can show up to three surfaces at the same time, defining more `blobs` which correspond to the chosen threshold values. The outer `blob` must be semi-transparent and white (this can be fixed with a `pigment` statement), the middle one semi-transparent and yellow, and the inner one red. This choice allows a white light ray to penetrate the first object; its yellow component is then partially reflected by the medium `blob`; finally the inner object reflects the red light.

Even if we have used colors to represent different surfaces, the images produced by POV-Ray can be converted to grey tones thanks to one of the many freeware tools available for this purpose nowadays. As an example, we present in Fig. 4 a grey tone picture showing three level of temperature during the nonlinear phase of the same kink instability discussed in Section 2.. Toroidal configuration, as defined in the Appendix, is used. Notice that the temperature is higher in the center, where a helicoidal current sheet, responsible for magnetic reconnection, is present.

This method is particularly attractive because it relies on a freeware tool for visualization. However POV-Ray requires conspicuous computer resources: it took about two hours on an HP 9000/730 workstation to produce Fig. 4.

## 4. Conclusions

Three dimensional MHD computations are used to simulate the physics of coronal loops in the Sun. In order to view and understand the results of our simulations, we have presented two imaging techniques. Even if they were developed for the visualization of MHD fields, those methods

---

<sup>1</sup>POV-Ray is available for many platforms. Source files and user’s documentation can be downloaded from the World Wide Web site <http://www.povray.org>.

are general enough to be applied to any vector field, whose field lines we wish to plot, and to any scalar field.

Thanks to the first technique, magnetic field lines can be viewed with any software capable of producing gray tone pictures. Gray tones are used because they are particularly apt to render a depth effect in three dimensional imaging. Moreover beautiful gray tone pictures are less expensive to print than average quality color pictures.

The second technique employs a freeware software to create multiple isosurfaces of three dimensional scalar fields. The only drawback of this method is the necessity of considerable computational resources for image rendering.

We believe that, combining the results obtained with the two procedures described in the present paper, we can reach a deeper comprehension of the physics driving the evolution of our system.

## 5. Acknowledgments

The author wishes to thank Prof. Antonio Messina, for reading a draft of the present paper and for his helpful suggestions. He is also deeply grateful to Dr. Roberto Casini for many discussions during the implementation of the methods here described and for proofreading the manuscript. Dr. Marco Velli kindly accepted to improve the English in the final version.

## 6. Appendix

We present here an optional procedure, applicable only to representations of coronal loops in cylindrical geometry. Although it does not alter the physics of our simulations, nonetheless we think it may ease confronting with observations. Before rearranging the points  $x_i^j$  as we have explained in Section 2., we remap them in a toroidal configuration. This provides the viewer with a more familiar scenario, in which loops have a natural curved shape. The transformation from toroidal (primed coordinates) to cylindrical (unprimed) configuration can be written as

$$\begin{aligned} x &= \sqrt{x'^2 + z'^2} - \frac{L}{\pi}, \\ y &= y', \\ z &= \frac{L}{\pi} \left( \arccos \frac{x'}{\sqrt{x'^2 + z'^2}} - \frac{\pi}{2} \right). \end{aligned} \quad (7)$$

Where  $L$  is the total length of the loop, extending from  $-L/2$  to  $L/2$  (see Fig. 1). The inverse transformation is

$$\begin{aligned} x' &= \left( x + \frac{L}{\pi} \right) \cos \pi \left( \frac{z}{L} + \frac{1}{2} \right), \\ y' &= y, \\ z' &= \left( x + \frac{L}{\pi} \right) \sin \pi \left( \frac{z}{L} + \frac{1}{2} \right). \end{aligned} \quad (8)$$

## 7. Literature

[BL96] A. J. C. Beliën, R. Leenders: *Comparison of Visualization Techniques and Packages (version 2.0)*, SARA visualization Center, downloadable from the World Wide Web site <http://www.sara.nl/Rik/REPORT.update/>, 1996

- [BPSLG96] A. J. Beliën, S. Poedts, H. J. W. Spolder, R. Leenders, J. P. Goedbloed: *Visualization of Resonant Absorption in Solar Coronal Loops by Simulation of Soft X-ray Images*, Computers in Physics, **10**, 1996
- [DA95] R. B. Dahlburg, S. K. Anthiochos: *Reconnection of Antiparallel Magnetic Flux Tubes*, Journal of Geophysical Research, **100**, 16991, 1995
- [ELV96] G. Einaudi, R. Lionello, M. Velli: *Magnetic Reconnection in Solar Coronal Loops*, Advances in Space Research, accepted for publication, 1996
- [GN96] K. Galsgaard, Å. Nordlund: *Heating and Activity of the Solar Corona 2. Kink Instability in a Flux Tube*, Journal of Geophysical Research, accepted for publication, 1996
- [LMS96] R. Lionello, Z. Mikić, D. D. Schnack: *Magnetohydrodynamics of Solar Coronal Plasmas in Cylindrical Geometry*, Journal of Computational Physics, submitted, 1996
- [P93] POV-Ray Team: *User's Documentation*, downloadable from the World Wide Web site <http://www.povray.org>, 1993
- [P82] E. R. Priest: *Solar Magnetohydrodynamics*, Reidel, Dordrecht, 1982
- [VLE96] M. Velli, R. Lionello, G. Einaudi: *Kink Modes and Current Sheets in Coronal Loops*, Solar Physics, accepted for publication, 1996